

Atomic structure and vibrational properties of icosahedral B₄C boron carbide

R. Lazzari,^{1*} N. Vast,^{1**} J.M. Besson,² S. Baroni,^{3,4+} and A. Dal Corso^{5†}

¹ CEA, Centre d'Etudes de Bruyères, 91680 Bruyères Le Châtel, France

² Physique des Milieux Condensés, UMR CNRS 7602, B77, Université P. et M. Curie, 4, Place Jussieu, 75252 Paris, France

³ Scuola Internazionale Superiore di Studi Avanzati and INFN, Via Beirut 2-4, 34014 Trieste, Italy

⁴ Centre Européen de Calcul Atomique et Moléculaire, ENS-Lyon, 46 Allée d'Italie, 69007 Lyon, France

⁵ Institut Romand de Recherche Numérique en Physique des Matériaux, EPFL, Ecublens, 1015 Lausanne, Switzerland

(August 27, 2018)

The atomic structure of icosahedral B₄C boron carbide is determined by comparing existing infra-red absorption and Raman diffusion measurements with the predictions of accurate *ab initio* lattice-dynamical calculations performed for different structural models, a task presently beyond X-ray and neutron diffraction ability. By examining the inter- and intra-icosahedral contributions to the stiffness we show that, contrary to recent conjectures, intra-icosahedral bonds are harder.

Covalently bonded solids based on boron, carbon, or nitrogen form the hardest materials presently known [1], and B₄C comes third after diamond and cubic BN, with the advantages of being easily synthesized and stable up to very high temperatures [2]. Hence it is used as abrasive or shielding material sustaining extreme conditions, while ¹⁰B-enhanced ceramics are used in nuclear reactors.

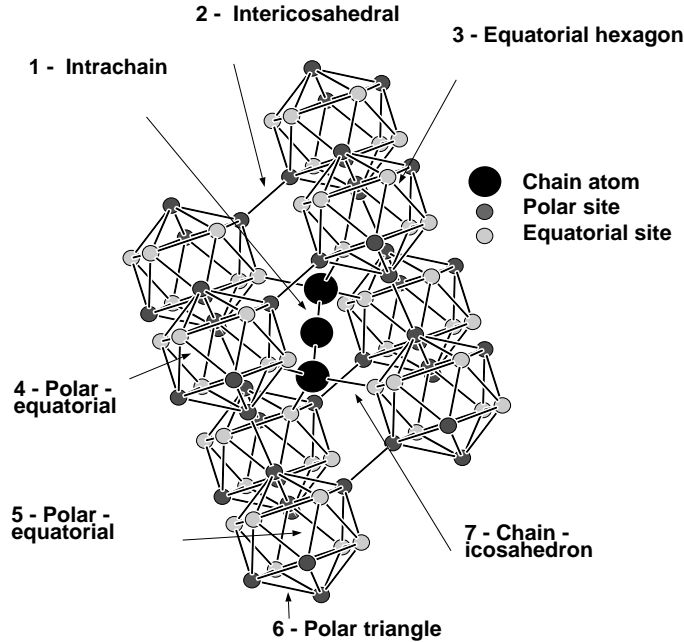


FIG. 1. Atomic structure of B₄C.

The atomic structure responsible for these properties is rather unique [3]: an arrangement of distorted B₁₁C icosahedra located at the nodes of a rhombohedral Bravais lattice ($R\bar{3}m$ space group, Fig. 1). This is a modification of the α -B₁₂ structure, which accommodates three-atom chains along the (111) rhombohedral axis, linking different B₁₁C icosahedra. Two inequivalent crystallographic sites exist in the icosahedron. The six atoms

which form the top and bottom triangular faces of the icosahedron sit at the *polar* sites, and are directly linked to atoms in neighboring icosahedra; the other six corners of the icosahedron form a puckered hexagon in the plane perpendicular to the $[111]$ axis, and their symmetry-equivalent sites are called *equatorial*. Each one of the six equatorial atoms is linked to an inter-icosahedral chain.

An experimental determination of the atomic structure of B_4C is still lacking [4,5]. Neutron diffraction [6,7] cannot distinguish ^{11}B from ^{12}C because their scattering lengths are too close [6]. X-ray diffraction has allowed to identify a C-B-C chain [8,9], but the location of the remaining C atom in the $B_{11}C$ icosahedron remains unsettled because the X-ray form factors of boron and carbon atoms are also too close. A recent attempt to resolve the atomic structure of B_4C using photo-emission and X-ray absorption spectra [5] did not yield conclusive results.

In this paper the determination of the atomic structure of B_4C is addressed by a combination of first-principles calculations, based on density-functional theory (DFT) and density-functional perturbation theory (DFPT), with infra-red absorption and Raman diffusion results. We have considered three ordered configurations of B_4C : in the *chain* configuration, all the icosahedra are entirely constituted by boron atoms— B_{12} —while all the carbon atoms lie entirely in the inter-icosahedral chains—C-C-C; in the *polar* configuration, the chains are assumed to be C-B-C, in agreement with X-ray diffraction data [8,9], while one of the polar atoms of the icosahedra is substituted by a carbon atom— $B_{11}C$; the *equatorial* configuration is similar to the polar one, but in this case the substitution involves an equatorial atom. These configurations are highly idealized, and some degree of substitutional disorder is expected to occur in actual samples. Nevertheless, their vibrational properties are sufficiently different so as to allow one to discriminate between different structural models by comparing the observed Raman and infra-red spectra with the predictions of accurate lattice-dynamical calculations. We finally determine the equation of state of B_4C and point out that the recently postulated *inverted molecular behavior* [10] is not consistent with our theoretical findings.

Calculations were performed within DFT and DFPT [11], using the local-density approximation and the plane-wave pseudo-potential method. The pseudo-potentials of boron and carbon were respectively the same as in Ref. [12] and [13]. Plane-waves up to a kinetic energy cutoff of 65 Ry have been included in the basis set. The irreducible wedge of the Brillouin zone has been sampled with 10 and 2 points for static and dynamic properties respectively in the chain model, and 20 and 3 points in the polar and equatorial ones. The structural parameters reported in table I have been obtained by minimizing the crystal energy with respect to the size, shape and internal degrees of freedom of the unit cell. The *chain* model has $R\bar{3}m$ symmetry, while the substitution of one B atom in the

TABLE I. Comparison between the structural parameters of B_4C as calculated for three structural models (*Chain*, *Polar*, *Equatorial*: see text) with those observed experimentally. a is the lattice parameter (Å), α is the angle between the rhombohedral lattice vectors (degrees), while b_n indicates the length of the n -th bond (Å) (see Fig. 1).

	<i>Chain</i>	<i>Polar</i>	<i>Equatorial</i>	Expt. ^a	Expt. ^b
a	5.12	5.10	5.13	5.163	5.155
α	65.9	65.8	64.9	65.732	65.679
b_1	1.30	1.42	1.43	1.434	1.438
b_2	1.70	1.71	1.69	1.716	1.699
b_3	1.73	1.73	1.72	1.693	1.687
b_4	1.77	1.78	1.78	1.758	1.760
b_5	1.77	1.77	1.77	1.762	1.761
b_6	1.81	1.78	1.78	1.805	1.810
b_7	1.65	1.59	1.59	1.675	1.669

^aRef. [8];

^bRef. [6].

icosahedron induces a small monoclinic distortion, which, for the polar and equatorial configurations, amounts to 1.8% and 0.5% of the rhombohedral cell length respectively, and to 1% and 0.1% of the rhombohedral angle respectively. The calculated data agree well with X-ray [8] and neutron diffraction [6] data (see Table I) for all of the three configurations. An agreement better than 3% is found for almost all of the bond lengths, which depend very little on the configuration. Exceptions to this are the intra-chain bond (bond #1 in Fig. 1) whose length would be underestimated by 10% in the chain model and the chain-icosahedron bond (bond # 7 in Fig. 1) which is predicted to be 5% too short both in the polar and the equatorial models. We interpret the failure to accurately predict the chain-icosahedron bond as due to our neglect of disorder effects in the chain. Occasionally, the chain could be B–C–C [7], a possibility which we did not consider. The calculated energies are also very close: those of B_{12} -CCC and equatorial B_4C are slightly higher by respectively 73 and 4 meV/atom as compared to polar B_4C which would then result to be the ground state. However, our neglect of disorder and of finite-temperature effects does not allow us to draw any definite conclusions.

In order to substantiate the hypothesis of a polar B_4C , we have decided to compare the vibrational spectrum predicted using state-of-the-art theoretical methods (DFPT) with that observed experimentally. As the difference of the atomic masses of boron and carbon amounts to 11%, one expects to observe a difference on those vibrational modes which involve mainly one of the two sites. In panels a-c of Fig. 2 we display the infrared spectrum as calculated for the three configurations and as deduced from reflectivity experiments [14]. The polarization-averaged absorption coefficient reads [15]:

$$\alpha(\omega) = \frac{2\pi^2}{3cn_1\Omega} \sum_j \sum_\alpha \left| \sum_{\beta s} Z_{\alpha\beta}^{*s} e_{\beta s}^j \right|^2 \delta(\omega - \omega_j), \quad (1)$$

where $Z_{\alpha\beta}^{*s}$ is the Born effective-charge tensor of s -th atom, c is the speed of light, Ω is the unit cell volume, α and β are Cartesian coordinates, j labels the vibrational mode, and ω_j , $e_{\beta s}^j$ the corresponding eigen-frequency and displacement pattern, respectively. For the polar and equatorial configurations, the dynamical matrix has been averaged with respect to all the symmetry-equivalent substitution sites in the icosahedron, so that rhombohedral symmetry is recovered also in these cases, and E_u (A_{2u}) modes are infrared active when light is polarized perpendicular (parallel) to the $[111]$ axis. Phonon lifetime and other broadening effects have been empirically accounted for by replacing the δ functions in Eq. (1) with Lorentzians with a half width of 10 cm^{-1} . The *positions* of the peaks agree only for the polar configuration.

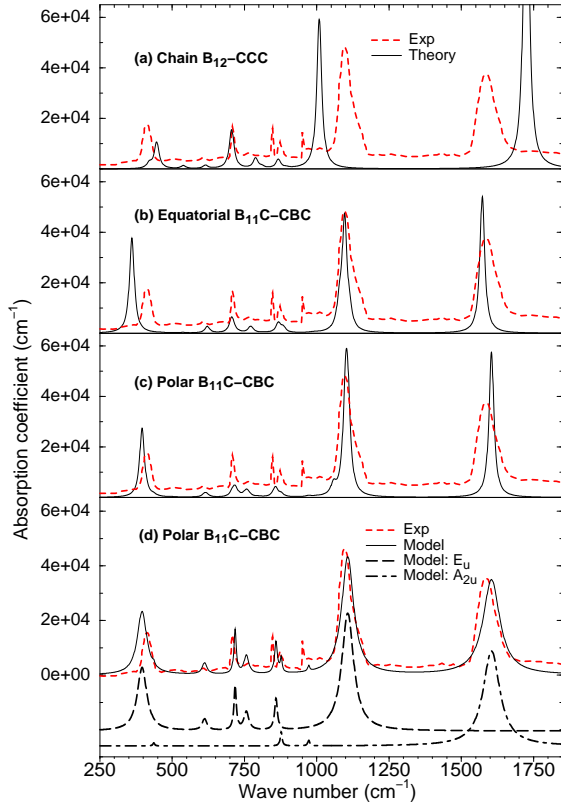


FIG. 2. Panels a-c: infrared spectra of B_4C as calculated for the three configurations considered in this work (solid lines) compared with that deduced from experiments [14] (dashed lines). (a) B_{12} -CCC; (b) equatorial B_4C ; (c) polar B_4C . Panel d: calculated spectrum of polar B_4C fitted to account for the experimental mixing of polarization. E_u (dash) and A_{2u} (dot-dash) contributions shifted for clarity.

The agreement between the calculated and observed peak *intensities* is still rather poor, mainly due to our

TABLE II. Polar B₄C: theoretical infrared active frequency ω (cm⁻¹) and relative integrated intensity I_{rel} . The highest intensity of each polarization is normalized to 10. Γ is the half width of the Lorentzians used in Fig. 2d (cm⁻¹).

E_u	ω	396	519	616	714	761	857	1103
	I_{rel}	4.1	$\approx 0.$	0.3	0.6	0.4	0.6	10.
	Γ	15.	5.	10.	5.	10.	3.	20.
A_{2u}	ω	436	720	877	972	1606		
	I_{rel}	0.1	$\approx 0.$	0.2	0.1	10.		
	Γ	4.	4.	4.	4.	30		

lack of knowledge of the individual line-widths as well as of the polarization conditions of the experiment with respect to the orientation of the sample. A simple adjustment of the theoretical data turns out to bring them in good agreement with experiments. We have re-weighted all the A_{2u} peaks with respect to the E_u ones by a same factor which is treated as a fitting parameter. Once this is done, we have kept the integrated intensity of each mode at its theoretical value, and we have utilized the widths of individual peaks as free parameters. The resulting values of the fitting parameters are reported in table II. The agreement between the experimental spectrum and the one predicted for the polar configuration is now very good (Fig. 2 d), and only the peak at 950 cm⁻¹ is missed by the theory. Its shape is asymmetric and its intensity varies from sample to sample [14,16], hence suggesting that it is not a simple bulk lattice vibration. In fact, theory predicts an infrared mode at 972 cm⁻¹ but its small intensity should hardly be observable (Table II). It might be activated by surface effects and/or bulk defects. Actually experiments are performed on hot-pressed micro-crystalline samples, where the defect density is very high. This leads to a degradation of the reflectivity spectrum with respect to the ideal (mono-crystalline) case, and the largest experimental error is expected at the LO minima.

In order to further confirm the polar configuration as the dominant one in B₄C, we now compare the Raman spectrum measured on a single crystal [17] with the predictions of our calculations (Fig. 3). Unfortunately, a complete quantitative comparison is difficult due to mode broadening, especially at high frequency. However, two modes at 481 and 534 cm⁻¹ are rather sharp [17], and they are properly accounted for only by the polar model, which predicts two peaks respectively at 498 and 543 cm⁻¹. The former is a rotation of the chain about an axis perpendicular to the [111] direction and the later is the librational mode of the icosahedron previously identified in α -boron [12]. These two modes have similar frequencies and widths, and they both involve angular atomic displacements, so that the errors made in the prediction of their positions are expected to be similar and to cancel to a large extent. The distance of 54 cm⁻¹ between

the two peaks is therefore a stringent test for the assignment, and only the polar configuration does account for it, while it is underestimated by a factor of two in the equatorial model (Fig. 3). At higher frequencies, structural disorder is likely to be responsible for most of the observed broadening. Twinning or stacking faults—recently identified as pairs of neighboring twin defects—are observed in single crystals [18]. They distort the crystal only slightly because they preserve the rhombohedral symmetry and the structure of the icosahedron. In B_4C ceramics obtained by hot pressing, however, these defects can be as close as a few lattice parameters [18], and the low-frequency part of the Raman spectrum is quite different from those of Fig. 3. In particular, while no Raman activity is expected in clean samples below 360 cm^{-1} , a broad band systematically appears at low frequency in ceramics [17,19], twice-peaked around 250 and 320 cm^{-1} , with an intensity which differs from sample to sample of a same bulk composition [17]. We attribute this band to a high density of states of disorder-activated acoustic phonons, in analogy to what is found, *e.g.*, in ice VII [20].

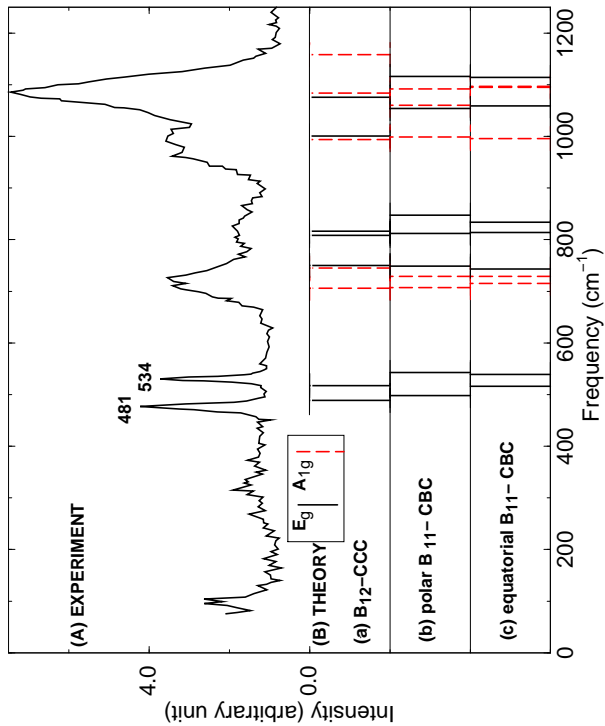


FIG. 3. B_4C Raman spectrum: (A) experiment [17] (B) theory for (a) $B_{12}\text{-CCC}$, (b) polar B_4C , (c) equatorial B_4C . Solid lines: E_g mode; dashed lines: A_{1g} mode.

Having shown that the vibrational spectra of B_4C can be consistently interpreted in terms of a carbon atom occupying one of the polar sites, we consider now its elastic properties, which have recently attracted some interest [10]. Theoretical volume *vs.* pressure data - determined up to a hydrostatic pressure of 10 GPa - have been

TABLE III. Theoretical and experimental bulk modulus (GPa) of the unit cell and of the icosahedron. Theoretical pressure derivatives are found to be: $B'_0=3.5$.

		This work	X-ray	Neutron	Ultrasound
B_4C	Unit cell	248	245 ^a	220 ^b	247 ^c
	icosahedron	274	-	169 ^b	-
α -boron	Unit cell	222	224 ^d		
	icosahedron	297	-		

^aRef. [22];

^bRef. [10];

^cRef. [21];

^dRef. [23].

fitted to a Murnaghan's equation of state: the resulting bulk modulus B_0 is reported in Table III together with the 'compressibility of the icosahedron' evaluated as in Ref. [10]. Our theoretical value is close both to ultrasonic measurements [21] and to unpublished X-ray data [22]. No evidence of the *inverted molecular behavior* reported in Ref. [10] was found from our calculations. In Ref. [10], a powder sample of NaCl and B_4C was used. Since the two materials have widely different elastic constants, they might have experienced very different pressures if, as it is often the case, some strain is transmitted at the grain boundaries (Voigt model). As no correction for this effect was made, the bulk modulus was probably found too low since at a given NaCl pressure (calibrant) the actual pressure experienced by B_4C was higher. For this reason the apparent bulk modulus of the icosahedra, which was found smaller than B_0 , might need to be verified in a quasi hydrostatic environment, with an accurate measurement of pressure. Moreover, twinning in boron allows the crystal to accommodate large strains and to prevent the formation of quasi-crystalline phases [18]. We are inclined to attribute the observed anti-molecular compression to pressure inhomogeneities induced by the intensive twinning in B_4C ceramics. An experiment on a single crystal would provide a definite answer to this issue.

In conclusion, the atomic structure of B_4C consists of one icosahedron $B_{11}C$ with the carbon atom staying at a polar site, and a chain C-B-C. B_4C and α boron are not molecular nor—as we have demonstrated—*inverted molecular* crystals. Rather, they should be considered as members of a new class of covalently bonded materials.

The authors are grateful to J. Loveday and D. Simeone for the communication of unpublished results. N.V. thanks L. Zuppiroli for a fruitful discussion.

* Presently at Laboratoire du Verre et des Interfaces, CNRS-SAINT GOBAIN, 93303 Aubervilliers, France.

- ** Author to whom correspondence should be sent. Electronic address: vast@bruyeres.cea.fr .
- + Electronic address: baroni@sissa.it .
- † Presently at SISSA, Trieste, Italy. dalcorso@sissa.it .
- [1] H. T. Hall and L.A. Compton, *Inorg. Chem.* **4**, 1213 (1965); S. Han, J. Ihm, S.G. Louie and M.L. Cohen, *Phys. Rev. Lett.* **80**, 997 (1998).
 - [2] I.J. McColm, *Ceramic Hardness*, Plenum press, New York (1990).
 - [3] J. Donohue, *The Structure of the Elements*, John Wiley and Sons, New York (1974).
 - [4] H. Werheit, U. Kuhlmann and T. Lundström, *Jour. of Alloys and Compounds* **204**, 197 (1994).
 - [5] I. Jiménez, D.G.J. Sutherland, T. van Buuren, J.A. Carlisle, L.J. Terminello and F.J. Himpsel, *Phys. Rev. B* **57**, 13167 (1998).
 - [6] B. Morosin B., G.H. Kwei, A.C. Lawson, T.L. Aselage and D. Emin, *Jour. of Alloys and Compounds* **226**, 121 (1995).
 - [7] G.H. Kwei and B. Morosin, *Jour. of Physical Chemistry* **100**, 8031 (1996).
 - [8] B. Morosin, T.L. Aselage and R.S. Feigelson, *Mat. Res. Soc. Symp. Proc.* **97**, 145 (1987).
 - [9] A.C. Larson, *Boron Rich Solids. Conf. Proc.* **140**, AIP, New York (1986), p. 109.
 - [10] R.J. Nemes, J.S. Lodevay, R.M. Wilson, W.G. Marshall, J.M. Besson, S. Klotz, G. Hamel, T.L. Aselage T.L. and S. Hull, *Phys. Rev. Lett.* **74**, 2268 (1995).
 - [11] S. Baroni, P. Giannozzi, and A. Testa, *Phys. Rev. Lett.* **58**, 1861 (1987); P. Giannozzi, S. de Gironcoli, P. Pavone, and S. Baroni, *Phys. Rev. B* **43**, 7231 (1991).
 - [12] N. Vast, S. Baroni, G. Zerah, J.M. Besson, A. Polian, J.C. Chervin and T. Grimsditch, *Phys. Rev. Lett.* **78**, 693 (1997).
 - [13] N. Troullier and J.L. Martins, *Phys. Rev. B* **43**, 1993 (1990).
 - [14] U. Kuhlmann, H. Werheit and K.A. Schwetz, *Jour. of Alloys and Compounds* **189**, 249 (1992). The absorption index has been obtained from the measured reflectivity spectrum using the Kramers-Krönig relation. From this we have then estimated the absorption coefficient by setting the real part of the refraction index to $n_1 = 2.7$, as its dependence on frequency is not known to us. This procedure does not affect the positions of the peaks and provides an estimate of the absorption coefficient within 10 to 20% which is precise enough for our purposes.
 - [15] P. Brüesch, *Phonons: Theory and Experiments II*, p. 50, Springer Verlag, Berlin (1986).
 - [16] H. Stein, T.L. Aselage and D. Emin, Ref. [21], p. 322.
 - [17] D.R. Tallant, T.L. Aselage, A.N. Campbell and D. Emin, *Phys. Rev. B* **44**, 2535 (1991).
 - [18] P. Favia, T. Stoto, M. Carrard, P.A. Stadelmann and L. Zuppiroli, *Micros. Microanal. Microstruc.* **7**, 225 (1996).
 - [19] D. Simeone, private communication (1997).
 - [20] J.M. Besson, M. Kobayashi, T. Nakai, S. Endo and Ph. Pruzan, *Phys. Rev. B* **55**, 11191 (1997).
 - [21] J.H. Gieske, T.L. Aselage and D.Emin, *Boron Rich Solids. Conf. Proc.* **231**, AIP, New York (1991), p. 377.
 - [22] J. Loveday, private communication (1997).
 - [23] R.J. Nemes, J.S. Lodevay, D.R. Allan, J.M. Besson, G. Hamel, S. Klotz, P. Grima and S. Hull *Phys. Rev. B* **47**,

7668 (1993).